MITSUBISHI ELECTRIC RESEARCH LABORATORIES
http://www.merl.com

On Parameter Identification of an Equivalent Circuit Model for Lithium-Ion Batteries

Tian, N.; Wang, Y.; Chen, J.; Fang, H.

TR2017-123 August 2017

Abstract

This paper focuses on nonlinear parameter identification of an equivalent circuit model for lithium-ion batteries (LiBs). A Thevenin's model is considered, which consists of a voltage source based on the battery's open-circuit voltage (OCV), an Ohmic resistor and two RC circuits connected in series. The objective is to identify all the parameters in the voltage source and circuits at once from the current-voltage data collected from a battery under constant-current discharging. Based on the voltage response, identifiability of the parameters is analyzed using the sensitivity analysis, and it is verified that the parameters are locally identifiable. An optimization problem based on nonlinear least squares is formulated to address identification, to which parameter bounds are imposed to limit the search space. The identification is then achieved by a trust region method. An evaluation based on experimental data illustrates the effectiveness of the proposed results. Differing from the existing work, this approach does not require an explicit relationship between the OCV and the battery's state- of-charge (SoC). Its application hence requires much less effort. Furthermore, the success in parameter identification can potentially contribute to parameter-analysis-based aging prognostics of LiBs.

IEEE Conference on Control Technology and Applications

On Parameter Identification of an Equivalent Circuit Model for Lithium-Ion Batteries

Ning Tian, Yebin Wang, Jian Chen and Huazhen Fang

Abstract— **This paper focuses on nonlinear parameter identification of an equivalent circuit model for lithium-ion batteries (LiBs). A Thevenin's model is considered, which consists of a voltage source based on the battery's open-circuit voltage (OCV), an Ohmic resistor and two RC circuits connected in series. The objective is to identify all the parameters in the voltage source and circuits at once from the current-voltage data collected from a battery under constant-current discharging. Based on the voltage response, identifiability of the parameters is analyzed using the sensitivity analysis, and it is verified that the parameters are locally identifiable. An optimization problem based on nonlinear least squares is formulated to address identification, to which parameter bounds are imposed to limit the search space. The identification is then achieved by a trust region method. An evaluation based on experimental data illustrates the effectiveness of the proposed results. Differing from the existing work, this approach does not require an explicit relationship between the OCV and the battery's state-of-charge (SoC). Its application hence requires much less effort. Furthermore, the success in parameter identification can potentially contribute to parameter-analysis-based aging prognostics of LiBs.**

I. Introduction

Lithium-ion batteries (LiBs), due to their high power density, long cycle life and low self-discharge rate, have become one of the most appealing ways for energy storage in sectors ranging from consumer electronics to electrified transportation and smart grid [1; 2]. Their increasing deployment has motivated an intense interest in the research of advanced LiB management, where the existing works are mostly focused on state-of-charge (SoC) and state-of-health (SoH) estimation [3–6], optimal charging strategy design [7–9], cell balancing [10], battery thermal management [11; 12].

Literature review. In the current literature, equivalent circuit models (ECMs) are widely used as a foundation for model-based estimation and control mentioned above, e.g., [13–16] and the references therein. An ECM is composed of resistors, capacitors and voltage sources to simulate a LiB's current-voltage dynamics. Its concise structure brings significant mathematical simplicity and amenability for use. While ECMs have gained much popularity nowadays, it is known that they must be explicitly available before being applied to the estimation and control tasks. This engenders the question of how to identify an ECM's parameters using a LiB's operation data (current, voltage, temperature, impedance spectroscopy, etc.).

The literature contains a few studies of solving this problem in an experimental context. For instance, the RC parameters are determined in [17; 18] through analyzing the transients in a LiB's voltage responses under certain excitations such as constant or pulse currents. The voltage source in an ECM typically represents the LiB's open-circuit voltage (OCV), which depends on the SoC. A parameterized SoC-OCV relationship can be identified by charging or discharging the LiB using a small current [19]. Though straightforward, these methods are empirical and ad-hoc rather than analytical, implying less accuracy. In the meantime, the experiments involved may not be time- or cost-effective. For instance, an SoC-OCV calibration experiment will take several hours, which is unaffordable in massive testing of LiBs. This thus has motivated research on more efficient data-driven parameter identification methods. In [20; 21], electrochemical impedance spectroscopy (EIS) data are fitted to an ECM to extract the resistance and capacitance parameters. In [22; 23], parameter identification based on the current-voltage data is addressed by an analytical method that reduces the problem of solving a set of high-order polynomial equations into one of solving several linear equations and a single-variable polynomial equation. A real-time identification algorithm is proposed for an ECM in [24], which comes with rigorous analysis of identifiability, convergence and identification bias. Associated with parameter identification, there is a growing amount of work on 1) optimal design of charging/discharging cycles to maximize the model identifiability [25; 26], 2) combined SoC and parameter estimation as a means of finding out SoC in the presence of unknown or time-varying battery parameters [5; 27–29]. These studies either assume an accurate SoC-OCV relationship available or impose approximations, e.g., OCV being piece-wise linear with SoC [29; 30] or constant during discharging [22; 23]. The practical truth, however, is that the OCV changes with SoC, sometimes dramatically, and is often difficult to accurately calibrate in practice.

Statement of contributions. This work sets its aim to address an interesting question: *will it be possible to identify all the parameters of an ECM in a one-stop procedure, including not only the ones for resistance and capacitance but also the ones in a parameterized SoC-OCV function?* A systematic development will be presented in this paper to derive a satisfactory answer. Here, the Thevenin's model is chosen and considered due to its wide and significant use.

N. Tian and H. Fang are with the Department of Mechanical Engineering, University of Kansas, Lawrence, KS 66045, USA {{ning.tian, fang}@ku.edu}.

Y. Wang is with the Mitsubishi Electric Research Laboratories, Cambridge, MA 02139, USA {yebinwang@merl.com}.

J. Chen is with the State Key Laboratory of Industrial Control Technology, College of Control Science and Engineering, Zhejiang University, Hangzhou 310027, China {jchen@zju.edu.cn}.

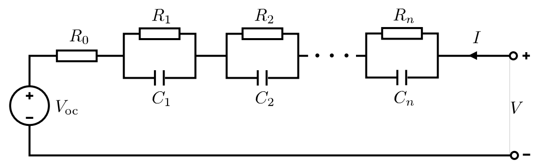

Fig. 1: A general-form Thevenin's equivalent circuit model.

An illustration of this model is shown in Figure 1, which includes an OCV source, an Ohmic resistor, and multiple serial RC circuits. With this choice, a constant current is assumed to be applied to fully discharge the LiB, with the resultant voltage response characterized. This then allows us to analyze the sensitivity of the output voltage with respect to the parameters to examine the identifiability of the involved parameters. The result shows that the model is indeed locally identifiable, implying the possibility of uniquely determining the parameters. Then, the parameter identification problem is posed from an optimization perspective to minimize the difference between model-based prediction and actual voltage response. The high nonlinearity of the optimization problem will risk parameter searches to local minimum physically meaningless. Hence, a set of constraints are imposed to limit the search space, based on some rough knowledge about the battery parameters. A trust region nonlinear least squares (NLS) method is then used to accomplish the search for optimal parameters. To summarize, the contribution of this work lies in the development of a systematic methodology for identifying all the parameters of the Thevenin's model. It only requires a very limited amount of prior knowledge about the battery. As a result, it can eliminate the need for a cumbersome experimental calibration of the SoC-OCV relationship, thus bringing considerable convenience in practice. This is the first study that we are aware of that can extract the parameters of the Thevenin's model all at once from the current-voltage data.

Organization. The rest of the paper is structured as follows. Section II introduces the Thevenin's model and its voltage response when excited by a constant discharging current. Section III begins with verifying the local identifiability of the unknown model parameters. It then proceeds to develop the NLS-based parameter identification procedure. Validation based on experimental data is offered in Section IV to demonstrate the efficacy of the proposed approach. Finally, Section V concludes the paper.

II. Problem Formulation

This section introduces the Thevenin's model to capture the behavior of LiBs in the case involving constant-current discharging and voltage recovering processes. An explicit relationship between the LiB's terminal voltage and the model parameters are derived, which will provide a foundation for identification in Section III.

Consider a general-form Thevenin's model as shown in Figure 1. This model comprises two parts: an OCV-based voltage source and RC components connected in series. Rather than fixed, the OCV changes with the SoC in a nonlinear manner during charging or discharging. Note that the SoC is defined as the ratio between a LiB's available energy and its nominal capacity, i.e.,

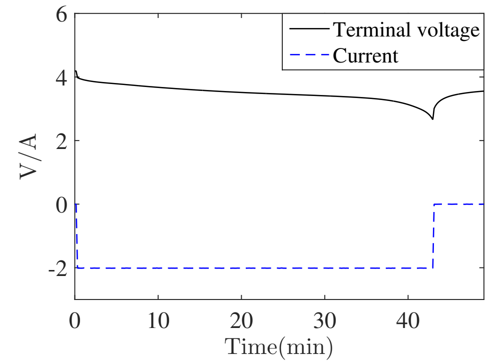

Fig. 2: The voltage response of a practical LiB in a full discharge experiment.

$$\dot{\mathrm{SoC}} = \frac{1}{3600Q} I, \tag{1}$$

where Q is the battery's nominal capacity in ampere-hour (Ah) and I is the current in ampere (positive for charging and negative for discharging). The RC circuits are used to emulate a LiB's transient behavior of the voltage response. The more RC circuits are used, the better the model can capture the transients of different time scales. However, two RC circuits, denoted as R_1-C_1 and R_2-C_2, are used in this paper as can offer sufficient model integrity and conciseness simultaneously which are verified in many works.

Based on Kirchhoff's circuit laws, the model equations can be expressed as

$$\begin{cases} \dot{V}_1 = -\dfrac{1}{R_1 C_1} V_1 - \dfrac{1}{C_1} I, \\ \dot{V}_2 = -\dfrac{1}{R_2 C_2} V_2 - \dfrac{1}{C_2} I, \\ V = V_{\rm oc} - V_1 - V_2 + R_0 I, \end{cases} \tag{2}$$

where V_1 and V_2 is the voltage across the R_1-C_1 and R_2-C_2 pairs, respectively, V the terminal voltage, and $V_{\rm oc}$ the OCV. As aforementioned, $V_{\rm oc}$ is dependent on SoC. Following [31; 32], it is parameterized as a fifth-order polynomial in SoC:

$$\begin{aligned} V_{\rm oc}(\mathrm{SoC}) = & \alpha_0 + \alpha_1 \mathrm{SoC} + \alpha_2 \mathrm{SoC}^2 + \alpha_3 \mathrm{SoC}^3 \\ & + \alpha_4 \mathrm{SoC}^4 + \alpha_5 \mathrm{SoC}^5, \end{aligned} \tag{3}$$

where α_i for $i = 0, 1, \ldots, 5$ are coefficients. It should be noted that $\alpha_0 = V_{\rm oc}(\mathrm{SoC} = 0)$, the OCV when the LiB is fully depleted. In addition, R_0 of many LiBs can vary significantly with SoC as suggested in the literature, e.g., [33–35], with the general trend of increasing with decreasing SoC. Hence, the relationship of R_0 and SoC in this work is parameterized

$$R_0(\mathrm{SoC}) = \beta_0 + \beta_1 e^{-\beta_2 \mathrm{SoC}}, \tag{4}$$

where β_i for $i = 0, 1, 2$ are another group of coefficients.

From above, (1)-(4) form the battery model. In this model, the parameters include α_i for $i = 0, 1, \ldots, 5$, β_i for $i =$

$0, 1, 2$, R_1, R_2, C_1 and C_2. Next, it will be of interest to determine how they relate to the voltage response. Consider that the battery is drained from full charge to full depletion by a constant current, which is then followed by a long enough rest period. Such a discharging process is likely the easiest to implement, thus often preferred in practice. An example of this process is taken from a real-world experiment conducted at NASA Ames Research Center, see Figure 2 and more details about the experiment in Section IV. It is seen that the terminal voltage V decreases through the discharging process. When the discharging ends, it jumps back due to the RC transients and gradually approaches a steady point.

Suppose that the battery has idled for a sufficiently long time, implying V_1 and V_2 at zero initially because C_1 and C_2 are uncharged. Then, the changes of V_1 and V_2 through time, respectively, are governed by

$$V_1(t) = IR_1 \left(1 - e^{-\frac{t}{R_1 C_1}}\right), \tag{5}$$

$$V_2(t) = IR_2 \left(1 - e^{-\frac{t}{R_2 C_2}}\right). \tag{6}$$

As a result, the terminal voltage during this process is

$$\begin{aligned} V(t) =& \alpha_0 + \alpha_1 \mathrm{SoC}(t) + \alpha_2 \mathrm{SoC}^2(t) + \alpha_3 \mathrm{SoC}^3(t) \\ &+ \alpha_4 \mathrm{SoC}^4(t) + \alpha_5 \mathrm{SoC}^5(t) + IR_1 \left(1 - e^{-\frac{t}{R_1 C_1}}\right) \\ &+ IR_2 \left(1 - e^{-\frac{t}{R_2 C_2}}\right) + I\beta_0 + I\beta_1 e^{-\beta_2 \mathrm{SoC}(t)}. \end{aligned} \tag{7}$$

If the rest period after the full discharge is long enough, V_1 and V_2 will approach zero, and V gradually recover and become equal to $V_{\rm oc}$. This implies that one can obtain $V_{\rm oc}(\mathrm{SoC} = 0)$, which is α_0. Hence, α_0 can be directly read from the final voltage measurement.

It is noticed that (7) fully defines the relationship between the terminal voltage V and the parameters α_i for $i = 1, \ldots, 5$, β_i for $i = 0, 1, 2$, R_1, R_2, C_1 and C_2. In sequel, it is assumed that these parameters are unknown, and the problem is how to identify from the measurements of V and I collected in a discharging cycle. However, prior to the identification procedure, one needs to decide if V is sensitive enough to a change in each parameter such that the data are informative enough to uniquely determine the parameters. This is known as identifiability analysis, which, together with the identification, is discussed in the next section.

III. Parameter Identification

This section presents the main results of this paper. It begins with investigating parameter identifiability by sensitivity analysis and then develops the identification algorithm.

A. Identifiability Analysis

A model structure is said to be identifiable if and only if its parameters can be uniquely determined from the input-output data. In other words, two different sets of parameter values should generate different output sequences under the same input for an identifiable model so that they can be distinguished from each other. It is shown in [27] that the local identifiability of a model can be tested by sensitivity analysis. Here, the sensitivity refers to the change of V with respect to the change of a parameter. To proceed further, we reformulate (7) for convenience of presentation as

$$V(t) = \phi(\boldsymbol{\theta}; t), \tag{8}$$

where $\boldsymbol{\theta}$ is the parameter set

$$\boldsymbol{\theta} = \begin{bmatrix} \alpha_1 \ \alpha_2 \ \alpha_3 \ \alpha_4 \ \alpha_5 \ R_1 \ \dfrac{1}{R_1 C_1} \ R_2 \ \dfrac{1}{R_2 C_2} \ \beta_0 \ \beta_1 \ \beta_2 \end{bmatrix}^\top,$$

and ϕ represents the mapping from $\boldsymbol{\theta}$ to V. Note that I is dropped for notational convenience because it is constant as aforementioned. It is noteworthy that $\boldsymbol{\theta}$ include $1/R_1C_1$ and $1/R_2C_2$ instead of C_1 and C_2. This is because the capacitance is at least three orders of magnitude larger than the resistance, which can introduce significant inaccuracy in numerical computation [36]. With the $\boldsymbol{\theta}$ selected as above, its elements are approximately at the same order of magnitude, advantageous for identification. In the remainder of the paper, $\boldsymbol{\theta}_i$ and its corresponding parameter will be used interchangeably.

The sensitivity of V with respect to the change of $\boldsymbol{\theta}$ can be characterized by the following matrix:

$$\boldsymbol{S}(\boldsymbol{\theta}) = \begin{bmatrix} \vdots & \vdots & \vdots & \vdots \\ \frac{\partial \phi(\boldsymbol{\theta}; t)}{\partial \boldsymbol{\theta}_1} & \frac{\partial \phi(\boldsymbol{\theta}; t)}{\partial \boldsymbol{\theta}_2} & \cdots & \frac{\partial \phi(\boldsymbol{\theta}; t)}{\partial \boldsymbol{\theta}_{12}} \\ \vdots & \vdots & \vdots & \vdots \end{bmatrix}, \tag{9}$$

where t corresponds to the sampling instants, and

$$\frac{\partial \phi(\boldsymbol{\theta}; t)}{\partial \boldsymbol{\theta}_i} = \mathrm{SoC}^i(t), \text{ for } i = 1, \cdots, 5, \tag{10a}$$

$$\frac{\partial \phi(\boldsymbol{\theta}; t)}{\partial \boldsymbol{\theta}_i} = I\left(1 - e^{-t\boldsymbol{\theta}_{i+1}}\right), \text{ for } i = 6, 8, \tag{10b}$$

$$\frac{\partial \phi(\boldsymbol{\theta}; t)}{\partial \boldsymbol{\theta}_i} = It\boldsymbol{\theta}_{i-1} e^{-t\boldsymbol{\theta}_i}, \text{ for } i = 7, 9, \tag{10c}$$

$$\frac{\partial \phi(\boldsymbol{\theta}; t)}{\partial \boldsymbol{\theta}_{10}} = I, \tag{10d}$$

$$\frac{\partial \phi(\boldsymbol{\theta}; t)}{\partial \boldsymbol{\theta}_{11}} = Ie^{-\mathrm{SoC}(t)\boldsymbol{\theta}_{12}}, \tag{10e}$$

$$\frac{\partial \phi(\boldsymbol{\theta}; t)}{\partial \boldsymbol{\theta}_{12}} = -I\mathrm{SoC}(t)\boldsymbol{\theta}_{11} e^{-\mathrm{SoC}(t)\boldsymbol{\theta}_{12}}. \tag{10f}$$

According to [27], $\boldsymbol{\theta}$ is locally identifiable if $\boldsymbol{S}(\boldsymbol{\theta})$ is of full rank. Hence, it is necessary to determine the independence between the columns. First, it is noted that columns 6 and 8, while taking a similar form as shown in (10b), would be independent of each other if $\boldsymbol{\theta}_7$ and $\boldsymbol{\theta}_9$ differ. It is interesting to note that $\boldsymbol{\theta}_7$ and $\boldsymbol{\theta}_9$ should be different practically because they are linked with RC transients at very different time scales. Given this, it is further seen that independence holds between columns 7 and 9 according to (10c). Finally, putting all the columns together and observing them, one can see that they are all linearly independent, verifying the full rankness of $\boldsymbol{S}(\boldsymbol{\theta})$. Thus, the parameter $\boldsymbol{\theta}$ is locally identifiable, paving the way for the identification procedure.

B. NLS-Based Parameter Identification

In light of (7)-(8), the identification of $\boldsymbol{\theta}$ can be considered from a data fitting perspective. As such, it can be achieved by minimizing the sum of squared residuals between the terminal voltage measurements and the model-based prediction. This will lead to an NLS problem. Meanwhile, a challenge arises from the nonlinearity and non-convexity of V with respect to $\boldsymbol{\theta}$. This implies the possibility that an optimization in an unconstrained space will approach a local minimum that is not physically meaningful. Therefore, it will be beneficial if the search is constrained within a reasonable space. Specifically, one can roughly determine the lower and upper bounds of $\boldsymbol{\theta}$ to set up a limited search space. It should be noted that this is not difficult practically, because some coarse-grained knowledge of a battery, e.g., internal impedance, can be obtained from both experience and some simple observation or analysis of the data. With this idea, the identification problem is formulated as

$$\min_{\boldsymbol{\theta}\in\mathbb{R}^n} f(\boldsymbol{\theta}) = \sum_{i=1}^{N} \left[V_i - \phi(\boldsymbol{\theta}; t_i)\right]^2, \tag{11a}$$

$$\text{s.t. } \underline{\boldsymbol{\theta}} \leq \boldsymbol{\theta} \leq \bar{\boldsymbol{\theta}}, \tag{11b}$$

where V_i is the terminal voltage measurement at the i-th time instant, N the total number of measurements, n the number of unknown parameters, and $\underline{\boldsymbol{\theta}}$ and $\bar{\boldsymbol{\theta}}$ the lower and upper bounds pre-set for $\boldsymbol{\theta}$, respectively. It is found that (11) represents an NLS problem. As a foundational problem in the area of optimization, NLS has received extensive research in the past decades, with prominent methods including line search algorithms and trust region algorithms. Here, a trust region method is considered [37]. For completeness, the following presents a brief overview of this method, which starts from the unconstrained case.

A trust region method is iteratively implemented. Take (11) as an example without considering the constraint (11b), and suppose that there is a current guess of the solution $\hat{\boldsymbol{\theta}}_k$, where k is the iteration step number. One can construct the following quadratic subproblem

$$\min_{\boldsymbol{s}\in\mathbb{R}^n} \psi_k(\boldsymbol{s}_k) = \boldsymbol{g}_k^\top \boldsymbol{s}_k + \frac{1}{2}\boldsymbol{s}_k^\top \boldsymbol{B}_k \boldsymbol{s}_k, \tag{12a}$$

$$\text{s.t. } \|\boldsymbol{D}_k \boldsymbol{s}_k\| \leq \Delta_k, \tag{12b}$$

where $\psi_k(\boldsymbol{s}_k)$ derives from the Taylor series of the objective function $f(\boldsymbol{\theta})$ at $\hat{\boldsymbol{\theta}}_k$, i.e., $\psi_k(\boldsymbol{s}_k) \approx f(\hat{\boldsymbol{\theta}}_k + \boldsymbol{s}_k) - f(\hat{\boldsymbol{\theta}}_k)$. In addition, $\boldsymbol{g}_k = \nabla f(\hat{\boldsymbol{\theta}}_k)$, $\boldsymbol{B}_k = \nabla^2 f(\hat{\boldsymbol{\theta}}_k)$, $\boldsymbol{D}$ a scaling matrix, $\|\cdot\|$ the Euclidean norm, and Δ the so-called trust region size. Here, (12) offers an approximate optimization problem that is "trusted" in a region centered around the current iterate $\hat{\boldsymbol{\theta}}_k$, and this region is the trust region. Solving it will gives an optimal $\boldsymbol{s}_k$, which is often called trial step. It is then interesting to see whether $\boldsymbol{s}_k$ can bring a large enough drop in $f(\boldsymbol{\theta})$ if added to $\hat{\boldsymbol{\theta}}_k$. A worthy metric is

$$\rho_k = \frac{f(\hat{\boldsymbol{\theta}}_k + \boldsymbol{s}_k) - f(\hat{\boldsymbol{\theta}}_k)}{\psi(\boldsymbol{s}_k)}, \tag{13}$$

TABLE I: Bound limits and initial guesses for $\boldsymbol{\theta}_6 - \boldsymbol{\theta}_{12}$ of batteries 5, 6, 33 and 34.

Name Unit	$\boldsymbol{\theta}_6$ Ω	$\boldsymbol{\theta}_7$ $1/(\Omega\mathrm{F})$	$\boldsymbol{\theta}_8$ Ω	$\boldsymbol{\theta}_9$ $1/(\Omega\mathrm{F})$	$\boldsymbol{\theta}_{10}$ Ω	$\boldsymbol{\theta}_{11}$ Ω	$\boldsymbol{\theta}_{12}$ 1
LB	0.05	0.0001	0.01	0.01	0.05	0.05	0.2
UB	0.5	0.002	0.5	0.1	0.5	0.5	100
Guess	0.1	0.001	0.1	0.1	0.05	0.3	35

Notation: LB lower bound, and UB upper bound.

where $f(\hat{\boldsymbol{\theta}}_k) - f(\hat{\boldsymbol{\theta}}_k + \boldsymbol{s}_k)$ is the actual reduction in $f(\boldsymbol{\theta})$, and $\psi(\boldsymbol{s}_k)$ the anticipated reduction. If ρ_k is greater than a threshold, then let $\hat{\boldsymbol{\theta}}_{k+1} = \hat{\boldsymbol{\theta}}_k + \boldsymbol{s}_k$, enlarge the trust region and continue the search. Otherwise, the trust region should be reduced, and rerun (12) at the same iterate point $\hat{\boldsymbol{\theta}}_k$.

In the case of (11b) applied as a constraint, there are different ways to cope with this, which share similar lines as above. An approach offered in [37] defines a new subproblem, in which $\psi_k(\boldsymbol{s}_k)$ is replaced by

$$\psi_k'(\boldsymbol{s}_k) = \boldsymbol{g}_k^\top \boldsymbol{s}_k + \frac{1}{2}\boldsymbol{s}_k^\top (\boldsymbol{B}_k + \boldsymbol{C}_k)\boldsymbol{s}_k, \tag{14}$$

where $\boldsymbol{C}_k$ is a matrix that accounts for the constraint. Similar to (12), this subproblem is then iteratively implemented to search for the optimal parameter estimate.

To conclude, this section verifies the local identifiability of parameters $\boldsymbol{\theta}$ by sensitivity analysis and establishes the parameter identification problem from the viewpoint of NLS-based data fitting. A constrained trust region method is then suggested to accomplish the identification. This design will be validated on experimental data in the next section.

IV. Experimental Results

In this section, the approach proposed in Section III is applied to an experimental data set to evaluate its efficacy in the real world.

The experimental data are from the Battery Data Set of NASA Ames Research Center [38]. The Battery Data Set contains many LiBs, which are classified into different subsets according to the discharging protocols. This work uses data collected from four batteries, which are numbered 5, 6, 33 and 34. Batteries 5 and 6 are from the same subset. They were discharged at a constant current of 2 A with the ambient temperature at 24°C. Batteries 33 and 34 are from another subset. They were discharged at a constant current of 4 A and under 24°C. Each battery was subjected to full charging/discharging in cycles. Here, cycle 431 for batteries 5, 6 and cycle 129 for batteries 33, 34 are considered, respectively. The discharging protocol presented in Figure 2 is cycle 431 conducted on battery 5, which was discharged from SoC = 1 to SoC = 0 under constant current of 2 A. Since batteries 6, 33 and 34 followed a similar discharging protocol, their discharging curves are omitted here.

To apply the aforeproposed approach, the bounds for the resistance and capacitance parameters are first set based on observation of the discharging data (no bounds are enforced for SoC-OCV parameters). An initial guess of the entire parameter vector is also picked. Here, all four batteries share the same bound setting and initial guess as collected in

TABLE II: Identified impedance parameters of Batteries 5, 6, 33 and 34.

Name	Cycle	R_1/Ω	C_1/F	R_2/Ω	C_2/F	β_0/Ω	β_1/Ω	$\beta_2/1$
Battery 5	431	0.181	3919	0.0435	851	0.0901	0.149	32.8
Battery 6	431	0.230	4058	0.0513	544	0.101	0.220	61.5
Battery 33	129	0.141	8199	0.0304	1315	0.127	0.187	59.7
Battery 34	129	0.0799	7895	0.0472	1416	0.137	0.144	38.6

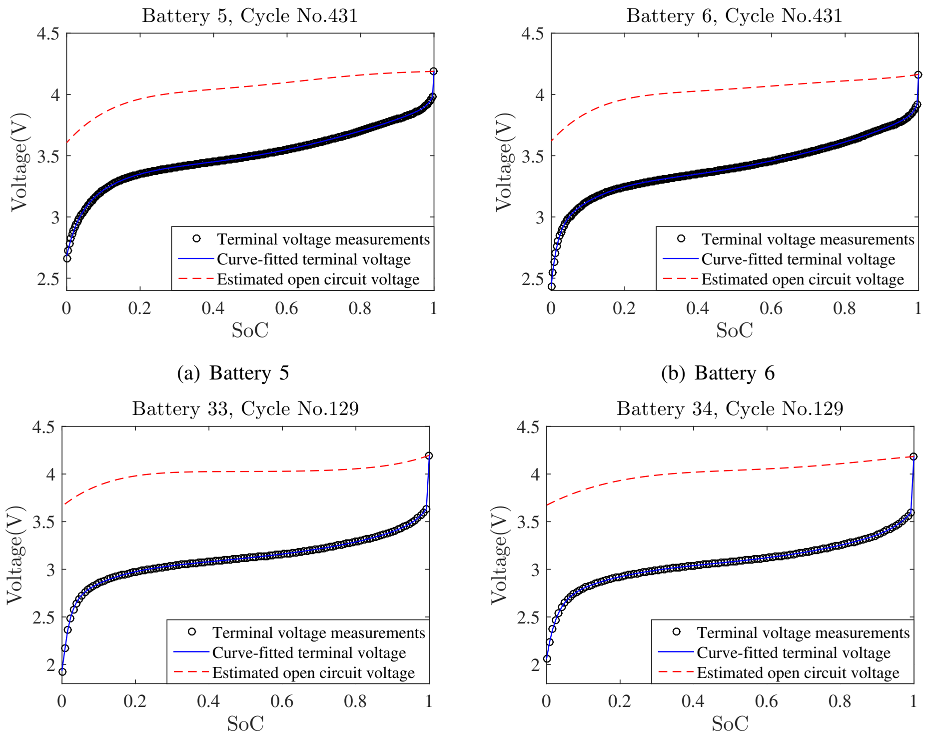

(a) Battery 5 (b) Battery 6

(c) Battery 33 (d) Battery 34

Fig. 3: Estimated SoC-OCV curves and actual/predicted terminal voltage comparison for batteries 5, 6, 33 and 34.

Table I. Following the procedure in Section III, the Matlab solver `lsqcurvefit` is leveraged to execute parameter search within the constrained space based on the trust region method. The resistance and capacitance parameters of all four batteries are shown in Table II. Based on experience with batteries, one can tell that the estimated parameters are physically reasonable. With the estimated SoC-OCV polynomial coefficients, the SoC-OCV relationship is reconstructed and presented in Figure 3. Meanwhile, it compares the actual terminal voltage with the one predicted using the parameter estimates, which exhibits an excellent agreement. The change of R_0 with respect to SoC has a significant influence on the battery's voltage behavior. Figure 4 depicts this for battery 5, revealing a much higher magnitude of R_0 at a low SoC level. This is the major contributing factor to the terminal voltage drop at a low SoC. Notice that this is different from some other types of LiBs that blame a significant drop in terminal voltage at a low SoC to the drop in OCV. But for the batteries considered here, their OCV at SoC=0 are relatively high (see Figure 2), the OCV jumps back to 3.6 V a long time after the discharging ends when the terminal voltage reaches 2.66 V. These observations suggest the reliability of the identification results and the promise of the proposed approach.

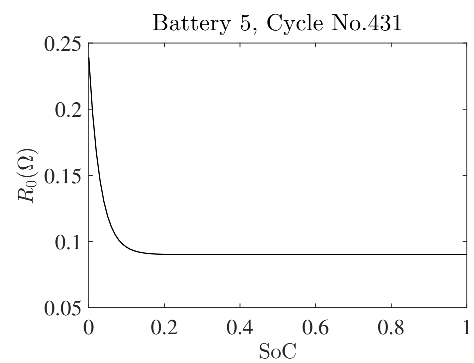

Fig. 4: Dependence of R_0 on SoC for battery 5.

V. Conclusion

This paper deals with nonlinear parameter identification of a Thevenin's model for LiBs. Despite the growth of LiB management research, model identification has received less attention even though it is the basis for various model-based management algorithms. The objective of this work is to build an easy-to-run approach to extract parameter estimates from the current-voltage data. Toward this end, the voltage response of a Thevenin's model in constant-current discharging is characterized, and then the parameter identifiability is analyzed through sensitivity analysis, which illustrates the parameters' local identifiability. An NLS-based identification problem is then posed, and numerical optimization based on a trust region method is proposed to solve it. The proposed approach is applied to identify the model of several batteries tested at NASA Ames Research Center, which produces effective identification results. The approach is based on a one-stop procedure and only requires a limited amount of, readily obtainable prior knowledge of a battery to set up the NLS search space. It is also applicable to battery data arbitrarily sampled in time. These advantages highlight the promise of this approach in LiB management practices. The results can be hopefully extended to analyze the cycle-based change of key physical parameters and track LiB aging, which will be our future work.

REFERENCES

[1] J.-M. Tarascon and M. Armand, "Issues and challenges facing rechargeable lithium batteries," *Nature*, vol. 414, no. 6861, pp. 359–367, 2001.

[2] M. Armand and J.-M. Tarascon, "Building better batteries," *Nature*, vol. 451, no. 7179, pp. 652–657, 2008.

[3] M. Coleman, C. K. Lee, C. Zhu, and W. G. Hurley, "State-of-charge determination from emf voltage estimation: Using impedance, terminal voltage, and current for lead-acid and lithium-ion batteries," *IEEE Transactions on Industrial Electronics*, vol. 54, no. 5, pp. 2550–2557, 2007.

[4] S. Lee, J. Kim, J. Lee, and B. Cho, "State-of-charge and capacity estimation of lithium-ion battery using a new open-circuit voltage versus state-of-charge," *Journal of Power Sources*, vol. 185, no. 2, pp. 1367–1373, 2008.

[5] H. Fang, X. Zhao, Y. Wang, Z. Sahinoglu, T. Wada, S. Hara, and R. A. de Callafon, "Improved adaptive state-of-charge estimation for batteries using a multi-model approach," *Journal of Power Sources*, vol. 254, pp. 258–267, 2014.

[6] H. E. Perez and S. J. Moura, "Sensitivity-based interval PDE observer for battery soc estimation," in *2015 American Control Conference*, 2015, pp. 323–328.

[7] C.-C. Lin, H. Peng, J. W. Grizzle, and J.-M. Kang, "Power management strategy for a parallel hybrid electric truck," *IEEE Transactions on Control Systems Technology*, vol. 11, no. 6, pp. 839–849, 2003.

[8] H. Fang and Y. Wang, "Health-aware and user-involved battery charging management for electric vehicles using linear quadratic control," in *ASME 2015 Dynamic Systems and Control Conference*. American Society of Mechanical Engineers, 2015, pp. V001T13A009–V001T13A009.

[9] Y. Wang, H. Fang, Z. Sahinoglu, T. Wada, and S. Hara, "Adaptive estimation of the state of charge for lithium-ion batteries: Nonlinear geometric observer approach," *IEEE Transactions on Control Systems Technology*, vol. 23, no. 3, pp. 948–962, 2015.

[10] Q. Ouyang, J. Chen, H. Liu, and H. Fang, "Improved cell equalizing topology for serially connected lithium-ion battery packs," in *2016 IEEE 55th Conference on Decision and Control*, 2016, pp. 6715–6720.

[11] Y. Hu, S. Yurkovich, Y. Guezennec, and B. Yurkovich, "Electro-thermal battery model identification for automotive applications," *Journal of Power Sources*, vol. 196, no. 1, pp. 449–457, 2011.

[12] X. Lin, H. E. Perez, S. Mohan, J. B. Siegel, A. G. Stefanopoulou, Y. Ding, and M. P. Castanier, "A lumped-parameter electro-thermal model for cylindrical batteries," *Journal of Power Sources*, vol. 257, pp. 1–11, 2014.

[13] R. Rao, S. Vrudhula, and D. N. Rakhmatov, "Battery modeling for energy aware system design," *Computer*, vol. 36, no. 12, pp. 77–87, 2003.

[14] M. Jongerden and B. Haverkort, "Battery modeling," Centre for Telematics and Information Technology, University of Twente, Tech. Rep., 2008.

[15] H. He, R. Xiong, H. Guo, and S. Li, "Comparison study on the battery models used for the energy management of batteries in electric vehicles," *Energy Conversion and Management*, vol. 64, pp. 113–121, 2012.

[16] X. Hu, S. Li, and H. Peng, "A comparative study of equivalent circuit models for li-ion batteries," *Journal of Power Sources*, vol. 198, pp. 359–367, 2012.

[17] B. Schweighofer, K. M. Raab, and G. Brasseur, "Modeling of high power automotive batteries by the use of an automated test system," *IEEE Transactions on Instrumentation and Measurement*, vol. 52, no. 4, pp. 1087–1091, 2003.

[18] S. Abu-Sharkh and D. Doerffel, "Rapid test and non-linear model characterisation of solid-state lithium-ion batteries," *Journal of Power Sources*, vol. 130, no. 1, pp. 266–274, 2004.

[19] V. H. Johnson, A. A. Pesaran, and T. Sack, "Temperature-dependent battery models for high-power lithium-ion batteries," National Renewable Energy Lab., Golden, CO (US), Tech. Rep., 2001.

[20] K. Goebel, B. Saha, A. Saxena, J. R. Celaya, and J. P. Christophersen, "Prognostics in battery health management," *IEEE Instrumentation & Measurement Magazine*, vol. 11, no. 4, 2008.

[21] C. Birkl and D. Howey, "Model identification and parameter estimation for $LiFePO_4$ batteries," in *Proceedings of IET Hybrid and Electric Vehicles Conference*, 2013, pp. 1–6.

[22] T. Hu, B. Zanchi, and J. Zhao, "Simple analytical method for determining parameters of discharging batteries," *IEEE Transactions on Energy Conversion*, vol. 26, no. 3, pp. 787–798, 2011.

[23] T. Hu and H. Jung, "Simple algorithms for determining parameters of circuit models for charging/discharging batteries," *Journal of Power Sources*, vol. 233, pp. 14 – 22, 2013.

[24] M. Sitterly, L. Y. Wang, G. G. Yin, and C. Wang, "Enhanced identification of battery models for real-time battery management," *IEEE Transactions on Sustainable Energy*, vol. 2, no. 3, pp. 300–308, 2011.

[25] S. Mendoza, M. Rothenberger, A. Hake, and H. Fathy, "Optimization and experimental validation of a thermal cycle that maximizes entropy coefficient Fisher identifiability for lithium iron phosphate cells," *Journal of Power Sources*, vol. 308, pp. 18 – 28, 2016.

[26] M. J. Rothenberger, D. J. Docimo, M. Ghanaatpishe, and H. K. Fathy, "Genetic optimization and experimental validation of a test cycle that maximizes parameter identifiability for a li-ion equivalent-circuit battery model," *Journal of Energy Storage*, vol. 4, pp. 156 – 166, 2015.

[27] H. Fang, Y. Wang, Z. Sahinoglu, T. Wada, and S. Hara, "State of charge estimation for lithium-ion batteries: An adaptive approach," *Control Engineering Practice*, vol. 25, pp. 45–54, 2014.

[28] H. He, R. Xiong, and H. Guo, "Online estimation of model parameters and state-of-charge of $LiFePO_4$ batteries in electric vehicles," *Applied Energy*, vol. 89, no. 1, pp. 413–420, 2012.

[29] H. Rahimi-Eichi, F. Baronti, and M.-Y. Chow, "Online adaptive parameter identification and state-of-charge coestimation for lithium-polymer battery cells," *IEEE Transactions on Industrial Electronics*, vol. 61, no. 4, pp. 2053–2061, 2014.

[30] C.-S. Huang and M.-Y. Chow, "Accurate Thevenin's circuit-based battery model parameter identification," in *Industrial Electronics (ISIE), 2016 IEEE 25th International Symposium on*. IEEE, 2016, pp. 274–279.

[31] A. Szumanowski and Y. Chang, "Battery management system based on battery nonlinear dynamics modeling," *IEEE Transactions on Vehicular Technology*, vol. 57, no. 3, pp. 1425–1432, 2008.

[32] C. Weng, J. Sun, and H. Peng, "A unified open-circuit-voltage model of lithium-ion batteries for state-of-charge estimation and state-of-health monitoring," *Journal of power Sources*, vol. 258, pp. 228–237, 2014.

[33] B. Y. Liaw, G. Nagasubramanian, R. G. Jungst, and D. H. Doughty, "Modeling of lithium ion cells—a simple equivalent-circuit model approach," *Solid State Ionics*, vol. 175, no. 1, pp. 835–839, 2004.

[34] M. Chen and G. A. Rincon-Mora, "Accurate electrical battery model capable of predicting runtime and IV performance," *IEEE Transactions on Energy Conversion*, vol. 21, no. 2, pp. 504–511, 2006.

[35] L. Lu, X. Han, J. Li, J. Hua, and M. Ouyang, "A review on the key issues for lithium-ion battery management in electric vehicles," *Journal of Power Sources*, vol. 226, pp. 272–288, 2013.

[36] A. Baba and S. Adachi, "Simultaneous state of charge and parameter estimation of lithium-ion battery using log-normalized unscented Kalman filter," in *American Control Conference (ACC), 2015*. IEEE, 2015, pp. 311–316.

[37] T. F. Coleman and Y. Li, "An interior trust region approach for nonlinear minimization subject to bounds," *SIAM Journal on Optimization*, vol. 6, no. 2, pp. 418–445, 1996.

[38] B. Saha and K. Goebel, "Battery data set," *NASA AMES Prognostics Data Repository*, 2007.